

Redox-Mediated Electrochemical Liquid-Liquid Extraction (ELLE) for the Continuous Molecularly- Selective Recovery of Critical Metals

*Stephen R. Cotty, Aderiyike Faniyan, Johannes Elbert, Xiao Su**

Department of Chemical and Biomolecular Engineering, University of Illinois Urbana-Champaign, 600 S Mathews Ave., Urbana, IL 61801, USA.

Corresponding Author

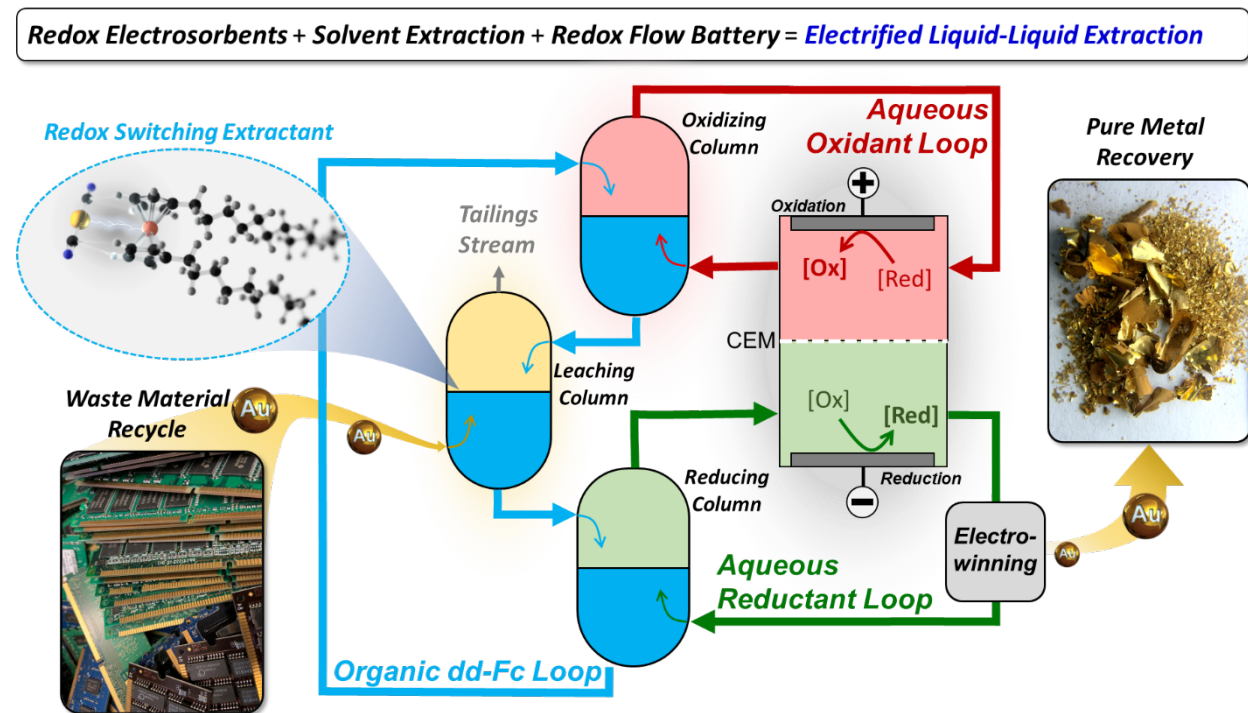
*Corresponding author. Email: x2su@illinois.edu

ABSTRACT

Selective electrochemical separations have become a powerful platform for the energy-efficient and modular extraction of critical elements, environmental remediation, and sustainable chemical manufacturing. However, the development of electroseparation technologies has primarily focused on heterogeneous adsorbents, all of which face the challenge of intermittent electroswing operation. For the first time, we present a unique redox-mediated approach for the selective recovery of critical materials, that translates selective single-site binding to a fully continuous separation scheme. Here, we propose a new separation architecture consisting of a fully continuous liquid-liquid extraction (LLE) scheme via the molecular design of a functionalized hydrophobic redox-active extractant. Our molecular design centers on tuning the chain length of the redox-moiety to control hydrophobicity and maximize organic phase retention, while preserving single site selectivity. Further, synergistic coupling of redox flow battery design enabled fully electrified redox-mediated LLE at continuous operation with no external chemical consumption to carry out the binding or release. We deploy the electrified liquid-liquid extraction (e-LLE) concept for the selective recovery of precious metals from dilute, contaminated metal leach solutions. The study demonstrates exceptional atomic efficiency of over 90% and over 100:1 selectivity in real-world critical metal leach streams, achieving fully continuous extraction and 16-fold up-concentration for gold and platinum group metals (PGMs) from electronic waste, catalytic converter waste, and mining streams. A techno-economic analysis highlights the significant

cost reductions of our electrified, continuous approach of precious metal recovery compared to conventional processes. Our work highlights a new design framework towards redox-mediated electrochemical separations that goes beyond surface-bound adsorption, and enables a sustainable, electron-transfer driven extraction method with higher scalability and the potential for addressing critical challenges in the circular economy for critical metals.

TOC GRAPHICS



Introduction.

Electrochemical separations offer a resource-efficient platform for critical metal recovery that can synergistically pair with a renewable energy infrastructure in a plug-and-play fashion¹⁻². Most notably, redox-mediated electro-sorbents have enabled unmatched ion uptake with tunable ion recognition, allowing highly selective and efficient purification of value-added chemical streams³⁻⁹. However, electrode-based adsorbent systems are inherently an intermittent process, necessitating frequent electrode regeneration stages to release the captured target species¹⁰, and ultimately limiting commercial viability and scalability. Translation to a fully continuous electrochemical process can bring transformative advantages for scalability and bring significant techno-economics benefits, as well as enhance direct applicability aligned with the growing trend for continuous industrial processes¹¹⁻¹². In this work, we demonstrate a new electrochemical design approach that uniquely unlocks a fully continuous operation of selective redox electro-separation. Through our proposed electrified liquid-liquid extraction (e-LLE) concept, we combine power of single site redox-mediated binding, with fundamental solvent extraction design principles, to enable a highly selective and efficient separation in a single, continuous unit operation.

Electrochemical separations have been proven as a viable approach to efficient and sustainable resource capture and purification¹³⁻¹⁴. By coating electrodes with redox-active materials, increased charge capacity and even selective ion capture has been demonstrated¹⁵⁻¹⁸, therefore marking a metamorphic change in electrochemical separations as a platform for

highly energy efficient purification of value-added materials¹⁹⁻²⁰. Redox-active polymer electrode coatings, such as polyvinyl ferrocene (PVF), have been demonstrated to enable the recycle of precious metal homogeneous catalysts *in-situ*, without destruction of the sensitive active catalyst structure, enabling extended turnovers¹⁹. Further, the redox-active ferrocene unit has shown a high affinity toward ionic gold complexes, unlocking one-step gold purification and refinement with unprecedented energy efficiency²⁰. Despite this, redox electrosorption schemes are intrinsically limited by the swing-nature of the adsorption process, and increasing system complexity often hinders the economy of scale needed for some of these critical element challenges¹⁰. While rocking chair-type designs have been investigated to enable pseudo-continuous operation of electrosorption,²¹ the increasing complexity of switching designs and performance losses can often negate the advantages of such schemes. Electrodialysis has long been an electrochemical separation platform with commercial success owing to its continuous operation, however viability is limited due to low target selectivity, high capital costs from membranes, and high operational costs from inefficiency²². Therefore, to this day electrochemical separations have been a tradeoff between target selectivity, energy efficiency, and scalability.

Liquid-liquid extraction (LLE) is a powerful and widely implemented technology in industry, especially for critical metal recovery, enabling efficient, scalable, and fully continuous chemical separation, particularly for critical metal recovery²³⁻²⁴. Sophisticated extractant chemistries have been developed to effectively capture aqueous precious metal

complexes into the organic extractant phase²⁵⁻²⁶. However, target metal release from the extractant phase (stripping) is intrinsically slow and chemically intensive with traditional extractants, relying on wasteful thermal or chemical swings to relinquish target from extractant, and thus historically limiting the economic viability of classical LLE as well as posing challenges to its sustainability²⁷⁻²⁹. To overcome these limitations and create a new framework towards electrified liquid-liquid extraction, our study proposes the utilization of a hydrophobic modified ferrocene unit as an electrochemically mediated extractant for the selective and efficient recovery of precious metals from dilute, contaminated metal leach solutions. Most critically, this redox extractant can be rapidly switched on and off with a mild electrochemical potential, resulting in the complete release and up-concentration of target species. Thus, this electrochemically switchable redox-extractant enables simple, continuous precious metal recovery with only electrical power.

The electrified liquid-liquid extraction (e-LLE) approach synergistically couples with renewable energy infrastructure, i.e. wind and solar, to form a fully sustainable metal recovery platform, in turn enabling sustainable recycling of resource intensive renewable technologies, perpetuating their economics. The ever-mounting climate crisis has led to unprecedented demand for valuable metals³⁰, and current supply is quickly falling short leading to a materials crisis in its own right³¹⁻³⁵. Precious metals like gold, platinum, palladium, and iridium, are some of the most environmentally damaging to mine owing to antiquated, energy intensive recovery technologies³⁶, and despite the high carbon footprint of refinement, these metals continue to

be extracted in larger quantities due to increasing demand³⁷⁻³⁹. Therefore this work investigates electrified liquid-liquid extraction (e-LLE) for fully continuous recovery of critical metals, namely gold, silver, copper, platinum, iridium, and rhodium to sustainably maintain a circular economy of these precious metals. Gold is used extensively in electronics⁴⁰, accounting for 8% of gold demand, and current recycling process are inefficient and environmentally polluting⁴⁰⁻⁴² with low economic viability⁴³⁻⁴⁴, leading to over 90% of gold in electronics sequestered to landfills in the US each year⁴⁵. Similarly, platinum group metals (PGMs) face great recovery challenges despite their low abundance and high technical demand as the pinnacle of catalytic materials⁴⁶. Currently, low supply of platinum and iridium bottlenecks economical green hydrogen production, being the critical material for efficient hydrogen fuel cells and electrolyzers⁴⁷. Therefore renewable methods of recovering these critical materials is paramount for sustainable future, and e-LLE may accomplish this renewably and economically.

This work tackles electrifying LLE with rational design, to produce a functionalized hydrophobic ferrocene redox-extractant with high binding affinity toward gold and PGMs. By increasing the functionalized hydrocarbon chain length, the Fc extractant was retained to the organic extractant phase with 0.5% loss to the aqueous phase. The resulting 1,1'-didodecylferrocene (ddFc) effectively extracted over 99% of aqueous gold into organic dichloromethane (DCM), demonstrating exceptional molecular efficiency (0.9 mol Au extracted for every mole of ddFc extractant) and selectivity. Selective gold uptake and up-

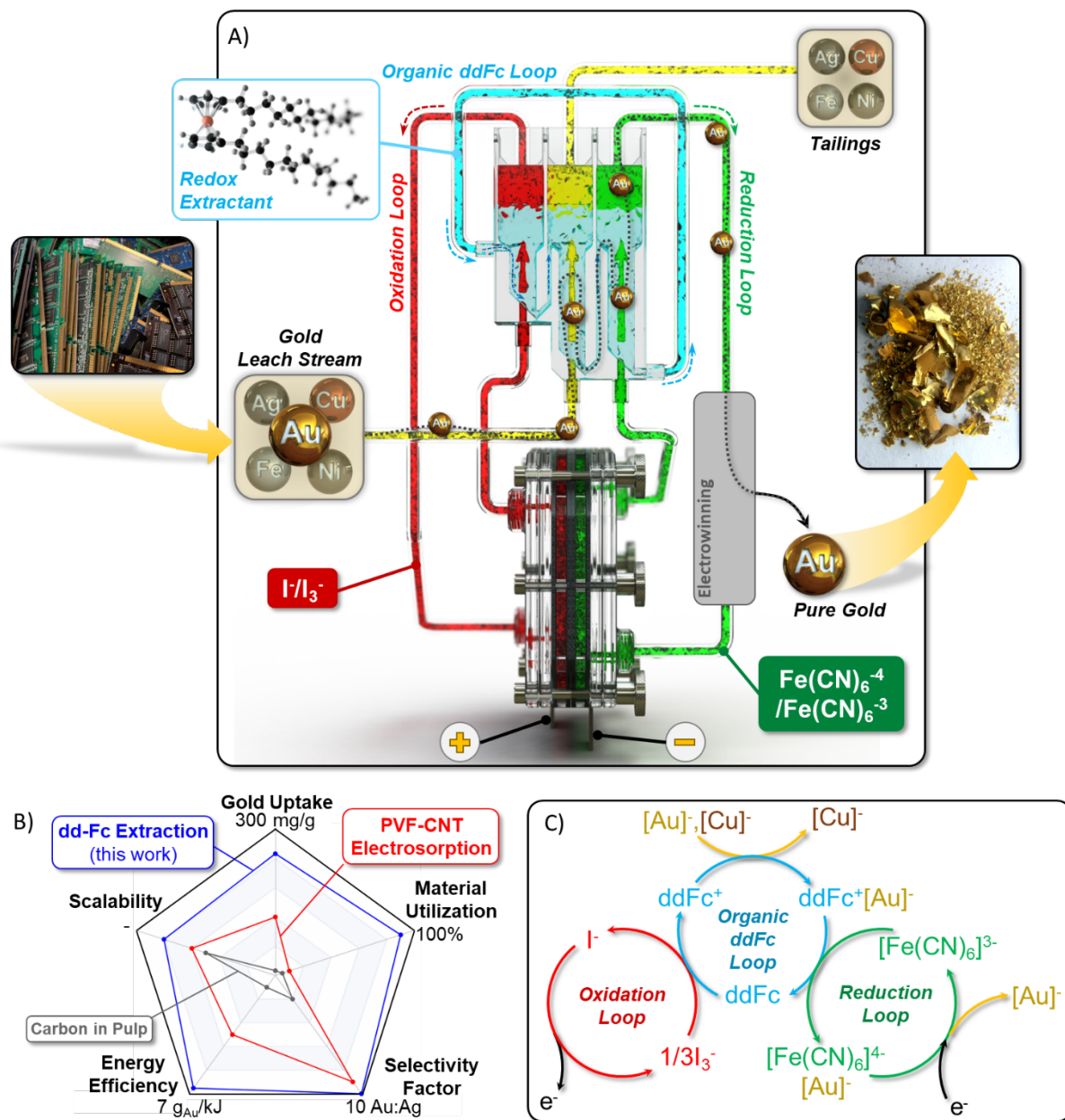


Figure 1. A) Schematic of the continuous e-LLE system consisting of three solvent extraction columns and a membrane-separated flow cell. B) overall comparison of the ddFc e-LLE extraction system (blue) to previous work (red) and the leading industrial technology (grey). Scalability refers to the system's ability to scale up and down. C) a detailed reaction schematic describing the e-LLE system consisting of three solution loops. In red is the aqueous oxidation loop with iodine. In blue is the organic extractant loop with ddFc in DCM. In Green is the aqueous reduction loop with ferrocyanide.

concentration were achieved in the e-LLE system in a fully continuous manner using practical gold leach solutions derived from local electronic waste and mining ore, with only electrical input. Additionally, extraction and purification of PGMs from automotive catalytic converter

material was conducted, and selective extraction of platinum and iridium chloro-complexes was achieved. A techno-economic analysis of the e-LLE system demonstrated significant cost reductions in gold recovery, making the economic recovery of previously unrecoverable ultra low-grade gold feasible. By simultaneously enhancing recovery performance and reducing energy and material consumption, the e-LLE process offers a new framework for the design of electrochemical separations, extending beyond membrane and adsorption based processes, and expanding its scope into highly scalable and adaptable liquid-liquid extraction processes for critical and precious metal recovery and purification.

Results and discussion

Electrochemical architecture design. A schematic of our electrified liquid-liquid extraction process (E-LLE) is shown in **Figure 1a** and **c**. Our approach uses a redox-active ferrocene-based extractant designed to remain sequestered to the organic phase, shown in blue. The organic extractant stream is looped through three consecutive solvent extraction columns: the oxidation, leach, and reduction column. 1,1'-didodecylferrocene (dd-Fc) extractant is activated via oxidation in the first column via an aqueous oxidizing agent, shown in red. From there, the oxidized dd-Fc in the organic stream contacts the aqueous gold-containing leach stream (yellow) in the second extraction column, and anionic dicyanoaurate, $[\text{Au}(\text{CN})_2]^-$, favorably binds to the oxidized dd-Fc extractant, selectively transferring the gold complex from the aqueous to the organic phase. The gold is reversibly released and concentrated into a new aqueous stream (in green) in the third and final extraction column. The dicyanoaurate anion

is liberated to the aqueous phase simply by reducing dd-Fc⁺ back to dd-Fc with an aqueous reducing agent, ferrocyanide. Pure metallic gold is efficiently recovered from the aqueous reducing loop (in green) via electrodeposition. The organic dd-Fc selective extractant can then be cycled back to the first extraction column and reused. Additionally, the oxidizing agent (in red) and reducing agent (in green) are simultaneously regenerated in a membrane-separated flow cell. Thereby achieving selective recovery and purification of gold continuously while only consuming electrical input.

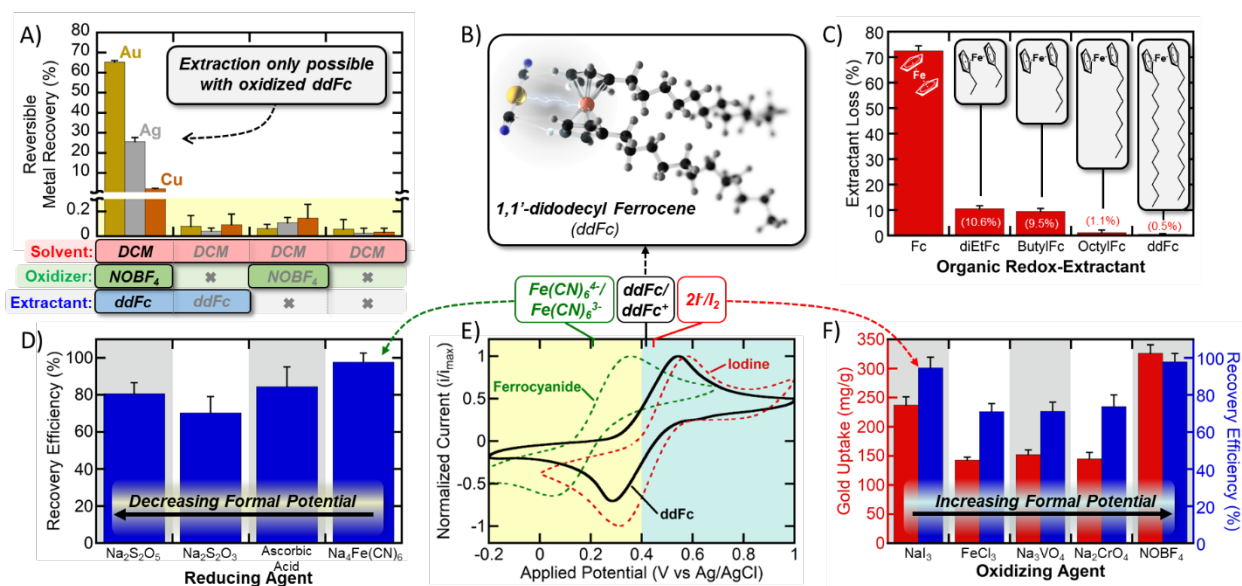


Figure 2. A) Comparison of control experiments for the recovery of gold (Au), silver (Ag), and copper (Cu), where reversible metal recovery is the percentage of metal released divided by the initial metal mass. All control experiments used DCM as organic phase solvents. Metal recovery is only observed when ddFc and NOBF₄ oxidizer are present. B) Rendering of oxidized ddFc⁺ binding to the dicyanoaurate anion. C) The percentage of ferrocene lost to the aqueous phase when oxidized as the hydrophobic tail is lengthened. 1,1'-didodecylferrocene (ddFc) had the least amount of loss. D) The recovery efficiency of gold for various aqueous reducing agents. For all experiments 2 mM of ddFc in DCM were oxidized with 2 mM NOBF₄ and mixed with 5 mM KAu(CN)₂. E) Cyclic voltammograms at a scan rate of 10 mV/s with carbon felt working and counter electrodes. The solution contained 10 mM aqueous sodium ferrocyanide for the green CV, and 10 mM aqueous sodium iodide for the red CV. The black CV was taken in a solution of DCM with 10 mM ddFc and 100 mM tetrabutylammonium hexafluorophosphate, and a leakless Ag/AgCl reference electrode was used. F) Gold uptake and release performance for various oxidizing agents.

Molecular design and selection of redox-mediated extractant. Redox-electrodes have previously been demonstrated to selectively bind to anionic cyano-gold via a directly applied oxidizing potential and reversible gold release when electrically reduced²⁰. Therefore, the ferrocene unit was selected as an effective organic extractant for E-LLE. An extractant must remain sequestered to the organic phase to be effective, and this was accomplished by functionalization of ferrocene (Fc) with a hydrophobic saturated hydrocarbon tail to Fc's cyclopentadiene ring. Once oxidized to ferrocenium (Fc⁺), the Fc site becomes highly hydrophilic and soluble in water (**Figure 2c**), thus to combat this phenomenon, the effect of increasing chain length functionalization on oxidized ferrocenium extractant was investigated with the aim to rationally design a highly hydrophobic ferrocene with less than 1% loss to the aqueous phase when oxidized. The loss of oxidized ferrocene from the organic dichloromethane (DCM) phase to the aqueous phase was determined with ICP-OES analysis for the following commercially available Fc functionalization's: Fc, 1,1'-diethylferrocene (diEtFc), and octylferrocene (OctFc). Additionally, ddFc was synthesized in house to provide a highly hydrophobic Fc and to gauge the economics of redox extractant production. Without functionalization, 42% of Fc was lost to the aqueous phase when oxidized (**Figure 2c**), and as the hydrocarbon side chain was lengthened, the ferrocene unit was more effectively sequestered to organic, with only 0.6% of dd-Fc lost after vigorous sonication of liquid phases. Therefore dd-Fc was chosen as the organic extractant for all following experiments.

A series of control gold extraction experiments were conducted to elucidate the mechanism of gold extraction from the aqueous phase to organic DCM phase (**Figure 2a**). Extraction of 5 mM $\text{KAu}(\text{CN})_2$ with pure DCM solvent resulted in negligible gold extraction (0.11% removal from aqueous) after vigorous shaking, and the addition of 2 mM reduced ddFc to the organic phase again resulted in negligible gold extraction (0.13% removal). However, oxidation of 2 mM ddFc in the organic phase with equimolar NOBF_4 oxidizer, resulted in 65.1% gold extraction to the organic phase after 10 seconds of vigorous shaking. A final control with only NOBF_4 in the organic phase (no ddFc) resulted in negligible gold extraction (0.13%), confirming that anionic gold extraction was only possible with the combination of ddFc and NOBF_4 oxidizer. An absorbance peak at 670 nm was observed in UV-Vis spectra of after gold extraction with both ddFc and NOBF_4 present, matching spectra of oxidized $\text{ddFc}(\text{III})^+$ (**Figure 3g**). Therefore, the active gold-binding species was oxidized ddFc^+ due to favorable charge transfer binding, in agreement with previously elucidated mechanisms of redox-site binding with metalloanion complexes²⁰.

System design rationale and redox mediator selection. Direct electrochemical redox of ddFc in organic DCM was possible with the addition of 100 mM tetrabutylammonium hexafluorophosphate supporting electrolyte (ddFc voltammogram shown in **Figure 2e**), however quaternaryammonium salts are known for increasing the miscibility of halogenated solvents with water and interfacial scum, resulting in chemical loss of solvents, ddFc extractant, and costly supporting electrolyte. To enable chemical-free extraction of gold, the

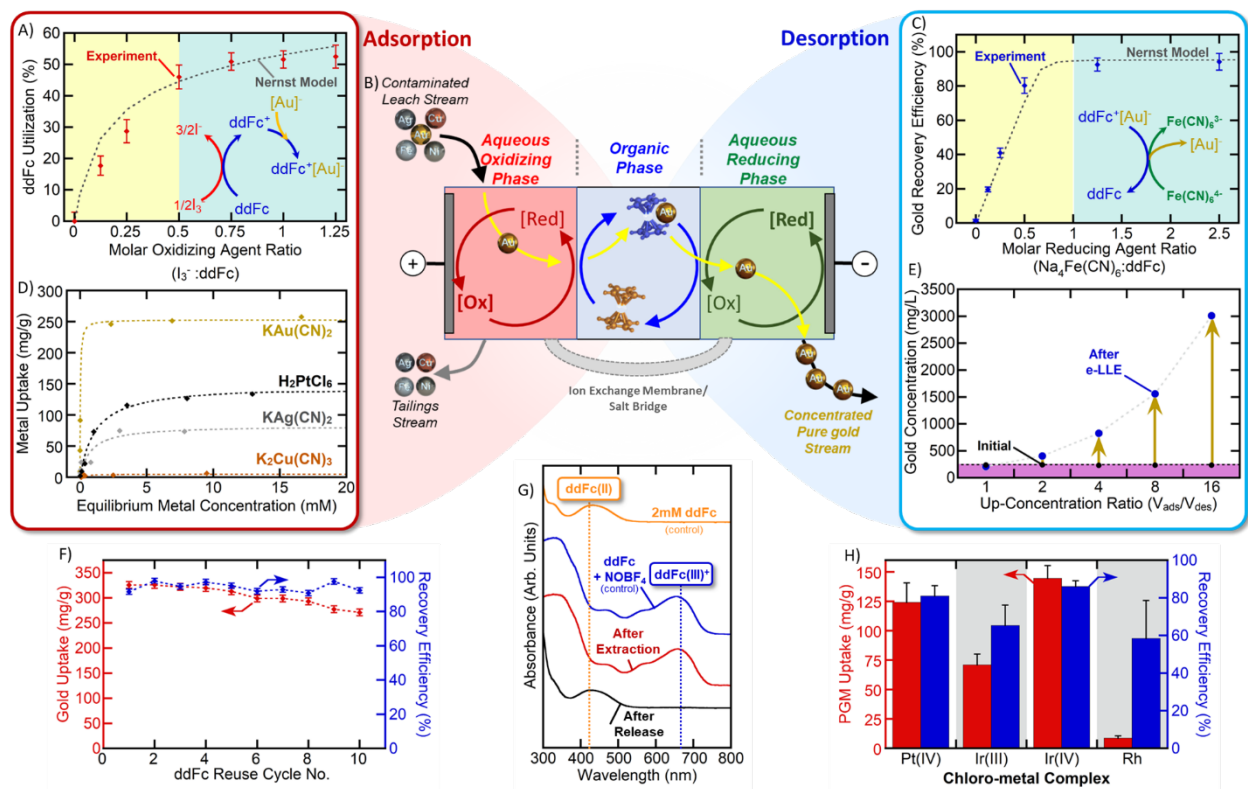


Figure 3. A) the molar utilization of ddFc as the molar ratio of aqueous triiodide oxidizer was increased for experimental data (red) compared to the Nernst model (grey line). B) schematic of the e-LLE system. C) gold recovery efficiency of gold extracted with ddFc oxidized with equimolar NOBF₄ as the molar ratio of aqueous ferrocyanide reducing agent was increased for experimental data (blue) compared to the Nernst model (grey). D) ddFc absorption isotherms for gold, silver, and copper. Experimental data are diamond points, and The Langmuir isotherm model was shown as a dashed line for each. E) gold recovery efficiency as a factor of the up-concentration ratio, set by decreasing the ratio of aqueous reducing solution to leach solution. As the volume of the reducing solution decreased, the gold was concentrated. F) ddFc cyclability study where the ddFc in DCM solution was recycled through 10 consecutive extraction and release cycles. G) UV-vis spectra of the organic extractant solution containing 2 mM ddFc in DCM before oxidation (orange), after oxidation and extraction (blue), and after reduction and release to aqueous (black). H) the uptake and release performance of ddFc extraction with H₂PtCl₆, Na₃IrCl₆, H₂IrCl₆, and Na₃RhCl₆.

organic ddFc extractant must be oxidized from Fe(II) to Fe(III) electrochemically. Therefore our design rationale centered on overcoming the low electrical conductivity of the organic phase ddFc extractant by indirectly switching the ddFc redox state via two aqueous-phase redox-mediators.

Aqueous triiodide can readily transform to diatomic iodine when exposed to organic solvent⁴⁸, and when applied to our E-LLE system, iodine oxidant was able to oxidize ddFc and achieved a high gold uptake of 237 mg/g (**Figure 2f**) with a very low, economical driving overpotential of 0.05 V ($E^{1/2} = 0.46$ V vs Ag/AgCl, **Figure 2e**). When the concentration of triiodide oxidant was varied from 0 mM to 5 mM (1.25 mol I_3^- per ddFc), an increase in gold uptake was observed with a maximum of 198 mg/g at 5 mM I_3^- , and experimental data matched the theoretical equilibrium Nernstian response ($R^2 = 0.98$) of 2-electron iodine reduction and 1-electron ddFc oxidation (**Figure 3a**). Therefore, ddFc oxidation with iodine was rapid, achieving equilibrium within 10 seconds. In the model, it was assumed that all oxidized ddFc⁺ would uptake an equimolar amount of anionic gold species, and this assumption was likely true, implying that molar utilization represents the percentage of ddFc oxidation for batch gold extraction results.

Reducing redox mediator selection. Electrochemical release of the target metal bound to oxidized ddFc⁺ in the organic phase was possible via reduction of ddFc⁺, and to accomplish this, an immiscible aqueous stream containing a suitable reversible redox species to mediate the reduction of ddFc had to be selected. 10 mM of common reducing agents were tested: Na₂S₂O₅, NaS₂O₃, ascorbic acid, and Na₄Fe(CN)₆ to recover gold extracted by 2 mM ddFc in DCM (oxidized with 2 mM NOBF₄). For sodium thiosulfate and sodium metabisulfite, 10 mM of NaOH was added to the aqueous reduction/release solution to ensure facile electron transfer⁴⁹. The resulting gold recovery efficiency (defined as the mass of released target species over mass

of extracted target, in percentage) from various reducing agents were shown in **Figure 2d**, and all reducing agents resulted in a color change in the organic phase from blue of ddFc^+ back to yellow of reduced ddFc . Sodium thiosulfate had the lowest recovery efficiency of 70.3%, followed by sodium metabisulfite (80%), and ascorbic acid (81%). Sodium ferrocyanide achieved nearly complete gold recovery at $97.7 \pm 1\%$, and the UV-Vis spectra of the ddFc -containing organic phase after desorption with ferrocyanide contained only one absorption peak at 420 nm, representative of reduced ddFc (**Figure 3g**). Gold was recovered from 2 mM ddFc^+ in DCM (with equimolar NOBF_4) using aqueous ferrocyanide of varying concentration (0 to 20 mM), and the resulting experimental gold recovery efficiency data was compared to a Nernstian equilibrium model in **Figure 3c**.

The gold recovery efficiency increased from 0% to 96% when the ferrocyanide: ddFc ratio was at unity and approached 98% with excess ferrocyanide, and the Nernst model captured experimental results well ($R^2 = 0.991$). Therefore, ferrocyanide rapidly reduced ddFc^+ to ddFc causing anionic dicyanoaurate to release from the organic phase and enter the aqueous ferrocyanide solution. The half-cell potential ferri/ferrocyanide redox couple was 0.21 V vs Ag/AgCl (**Figure 2e**). Due to its high recovery performance, moderate reduction potential, and electrochemical reversibility, sodium ferrocyanide was used at the redox couple to reduce ddFc^+ for all gold capture and release experiments in this work.

e-LLE performance with gold. A gold absorption isotherm was constructed using 2 mL of 2 mM ddFc in DCM oxidized with equimolar NOBF_4 , and 1 mL of an aqueous $\text{KAu}(\text{CN})_2$ solution

with concentration ranging from 0.1 mM to 20 mM. Gold extraction was carried out after shaking both immiscible liquids in a sealed vial for 10 seconds, and the gold-laden organic phase was transferred to a new vial containing 1 mL of aqueous 10 mM $\text{Na}_4\text{Fe}(\text{CN})_6$ to reduce ddFc and relinquish the captured gold to the aqueous reduction solution. The same process was carried out for extraction targets $\text{KAg}(\text{CN})_2$ and $\text{K}_2\text{Cu}(\text{CN})_3$, and the resulting reversible uptake isotherms showed favorability to gold followed by silver, with negligible uptake of copper (**Figure 3d**), agreeing with trends from our previous work with PVF-CNT electrodes.

For gold, the Langmuir isotherm model fits experimental results well ($R^2 = 0.992$) with Q_{max} of 253 $\text{mg}_{\text{Au}}/\text{g}_{\text{ddFc}}$ and an equilibrium coefficient, $K_{\text{eq}} = 39.4 \text{ mM}^{-1}$ (**Figure 3d**). Gold uptake rapidly approached a maximum beyond a gold concentration of 0.2 mM indicating that dicyanoaurate-ddFc binding was extremely favorable (**Figure S22a**). Below a concentration of 0.2 mM, over 99% of gold was removed in a single extraction pass, and above 0.2 mM, 81% of ddFc were utilized for the uptake of gold, proving ddFc as a high-performance gold extractant with incredible atom efficiency (**Figure S22b**). When the concentration of ddFc in the organic phase was varied from 1 mM to 20 mM with the concentration of aqueous $\text{KAu}(\text{CN})_2$ held constant (10 mM), the resulting gold absorption isotherm matched the Langmuir model well (**Figure S23**), confirming that Langmuir absorption fully captures the gold-ddFc extraction equilibrium regardless of gold and ddFc concentration.

Over a range of gold concentrations from 0.1 to 20 mM (**Figure S24**), and ddFc concentrations from 1 mM to 20 mM (**Figure S25**), gold capture was highly reversible, with

over 90% recovery efficiency. 2 mM ddFc in DCM was reused over 10 extraction and release cycles of 5 mM $\text{KAu}(\text{CN})_2$, and gold uptake remained consistently high (avg. 304 mg/g) with a slight loss of utilization from 86% to 72% by the 10th reuse cycle (**Figure 3f**), which may be accounted for by losses in liquid handling in the batch process. Gold recovery efficiency, however, remained consistently high (avg. 94%), indicating that ddFc was successfully regenerated each cycle and capable of repeated turnover.

Up-concentration of gold with the ddFc E-LLE system was investigated by changing the volume ratio of aqueous leach and aqueous release solution from 1:1 to 16:1 for a theoretical gold up-concentration ratio of 16. After extracting 1 mM $\text{KAu}(\text{CN})_2$ with 2mM of oxidized ddFc⁺ in DCM and releasing the organic-bound gold into aqueous ferrocyanide solution, the gold recovery efficiency was 97±4% for all up-concentration ratios of gold (**Figure S26**). Extraction of 235 mg/L of gold from a 16 mL solution and subsequent desorption to a 1 mL solution yielded a final gold concentration of 3012±7 mg/L (**Figure 3e**) with a recovery efficiency of 92%, demonstrating that up-concentration was possible with the e-LLE system.

Multi-component selectivity performance. Absorption isotherms were constructed for $\text{KAg}(\text{CN})_2$ and $\text{K}_2\text{Cu}(\text{CN})_3$ over a range of concentrations from 0.1 mM to 20 mM with 2 mM ddFc in DCM oxidized with equimolar NOBF_4 , and the reversible uptake isotherms of silver and copper were compared to gold in **Figure 3d**. Silver uptake with ddFc was highly irreversible with an average recovery efficiency of 35%, indicating that ddFc extraction was not the major mechanism of silver removal. From control experiments, silver extraction only

occurred with oxidized ddFc⁺ (**Figure 2a**). Therefore, oxidized ddFc⁺ was necessary for silver removal, however binding of the Ag(CN)₂⁻ to ddFc⁺ in DCM solvent may have resulted in decomposition of the silver complex to AgCN, which is insoluble in water⁵⁰. The reversible uptake isotherm for silver did fit the Langmuir absorption isotherm model ($R^2 = 0.97$) with Q_{\max} of 83 mg/g and K_{eq} of 1.2 mM⁻¹, indicating that ddFc-silver binding did occur. When compared to dicyanoaurate absorption isotherm in **Figure 3d**, uptake of anionic dicyanoargentate ([Ag(CN)₂]⁻) was indeed unfavorable with ddFc, despite the structural similarities between cyano- silver and gold complexes. In a binary mixture of 5 mM KAu(CN)₂ and 5 mM KAg(CN)₂, the selectivity factor of gold extraction with ddFc, relative to silver, was 18.5:1 (**Figure S27**), confirming the favorability of gold-ddFc binding over silver.

Copper uptake with ddFc was largely irreversible with an average recovery efficiency of 15% and a maximum reversible uptake of 6.4 mg_{Cu}/g_{ddFc} at 10 mM K₂Cu(CN)₃ (**Figure S28**), therefore copper binding to ddFc⁺ was highly unfavorable. From control experiments, copper extraction only occurred with oxidized ddFc⁺ (**Figure 2a**), indicating that copper indeed interacted with ddFc⁺, albeit to a small degree (1% extraction). Binary extraction of 5 mM gold and 5 mM copper resulted in a high gold selectivity factor of 113:1 relative to copper, as expected (**Figure S29**). For stability of the cyano-copper complex, 5 mM KCN was present in the aqueous leach solution, and therefore the effect of excess free cyanide (KCN) in the metal leach was investigated with 5 mM KAu(CN)₂ as the target metal. The uptake of gold was observed to progressively decrease from 301 to 165 mgAu/g_{ddFc} as the concentration of KCN

increased from 0 to 10 mM, however gold recovery efficiency remained consistently high with an average of 90% (Figure S30). From literature, free cyanide (CN^-) can be oxidized to $(\text{CN})_2$ above a formal potential of 0.35V vs Ag/AgCl⁵¹. Therefore, excess free cyanide likely caused premature reduction of ddFc^+ , with a formal potential of 0.41 V vs Ag/AgCl, resulting in lower gold uptake. However, a great excess (>10 mM) of free cyanide was required to appreciably

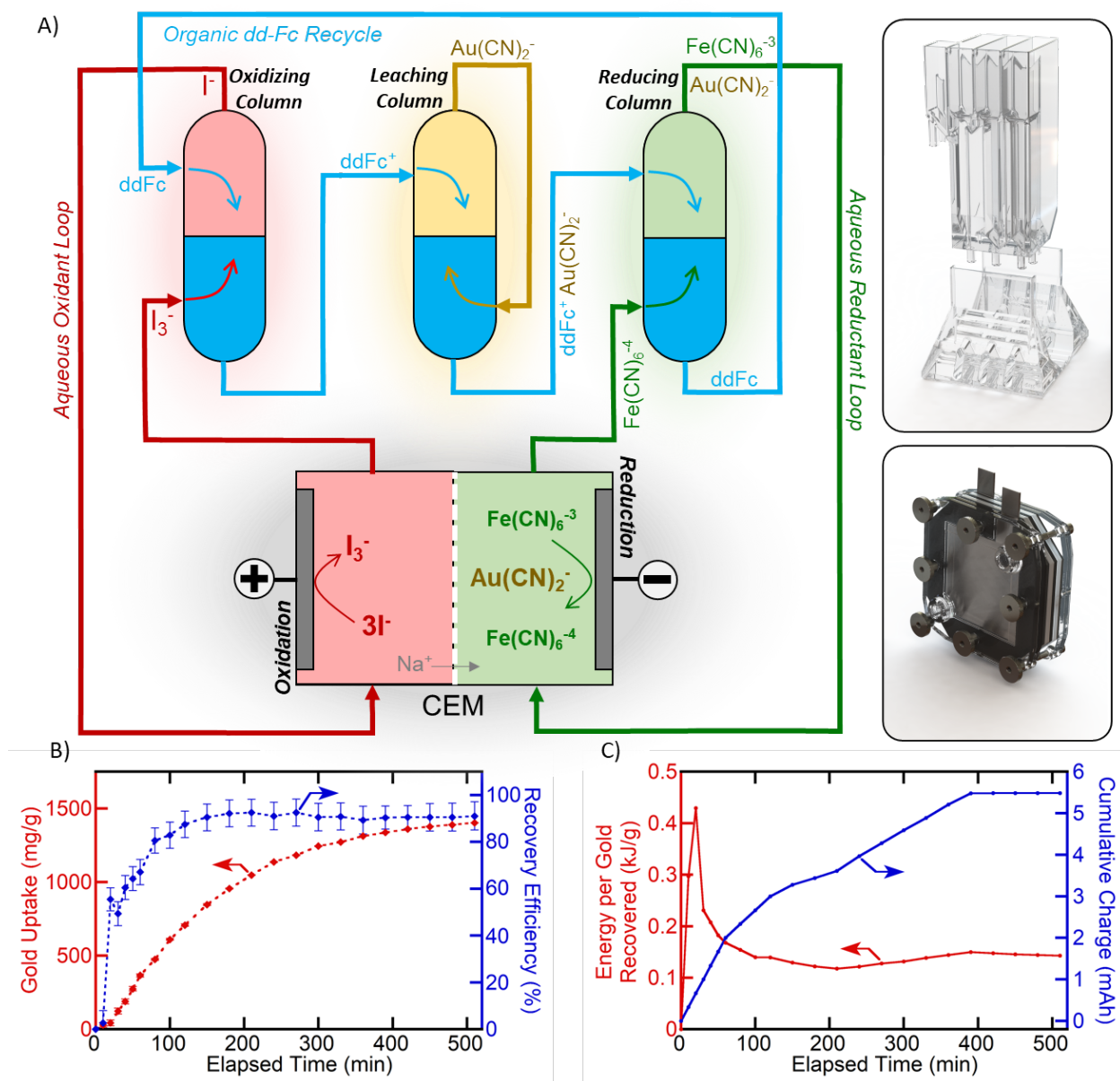


Figure 4. A) schematic of the continuous flow e-LLE system used for continuous flow extraction experiments. B) continuous e-LLE uptake and gold recovery performance kinetics, where the system achieved 1402 mg/g uptake and 92% recovery simultaneously. C) Energy consumption normalized by the mass of gold that was recovered and cumulative charge over time for the flow cell as it regenerated oxidizer and reductant.

reduce ddFc^+ , and 5 mM of free KCN resulted in only a 13% loss in gold uptake. As such, it is recommended that the free cyanide concentration of a metal leach solution should be less than 5 mM.

PGM recovery performance. Extraction of various anionic chloro-complexes of platinum group metals (PGMs) were tested with ddFc e-LLE: $[\text{Pt(IV)Cl}_6]^{2-}$, $[\text{Ir(III)Cl}_6]^{3-}$, $[\text{Ir(IV)Cl}_6]^{2-}$, and $[\text{Rh(III)Cl}_6]^{3-}$. For each species, 5 mM of aqueous PGM was extracted into DCM by 2 mM ddFc oxidized with equimolar NOBF_4 , and subsequently released to a new aqueous reduction stream containing 10 mM sodium ferrocyanide for complete reversible extraction. Pt(IV) and Ir(IV) showed the highest uptakes ($124 \text{ mg}_{\text{Pt}}/\text{g}_{\text{ddFc}}$ and $144 \text{ mg}_{\text{Ir}}/\text{g}_{\text{ddFc}}$) and the highest separation reversibility of 81% and 86% respectively (**Figure 3h**). The uptake of Ir(III) was only $71 \text{ mg}_{\text{Ir}}/\text{g}_{\text{ddFc}}$ – half that of Ir(IV), and virtually no Rh(III) was extracted by ddFc (**Figure 3h**). These findings suggest that ddFc-enabled extraction most favorably extracts anionic metal complexes of increasing atomic size, i.e., $\text{Au} > \text{Pt} \sim \text{Ir} > \text{Ag} > \text{Ru} > \text{Cu}$, and uptake decreases as the formal charge of the target anion becomes more negative, i.e., $[\text{Au(CN)}_2]^- > [\text{PtCl}_6]^{2-} > [\text{IrCl}_6]^{3-}$. A reversible uptake isotherm was made for chloroplatinic acid, and the Langmuir isotherm model was fit ($r^2 = 0.988$) with $Q_{\text{max}} = 148 \text{ mg/g}$ and $K_{\text{eq}} = 0.88 \text{ mM}^{-1}$ (**Figure 3d and Figure S31**). Notably, the Q_{max} of $[\text{PtCl}_6]^{2-}$ was roughly half of the Q_{max} for $[\text{Au(CN)}_2]^-$, and this is likely due to the Pt complex's formal charge of 2-, requiring two ddFc⁺ units to extract a single Pt species.

Aqueous PGMs were mixed with pure solvents, DCM, chloroform, hexane, and xylene, to understand background uptake due to PGM-organic solubility, and only 4.1% of aqueous

PGM salts leached to the organic DCM phase on average (**Figure S32**). Pt(IV) and Ir(IV) complexes were the most soluble in all organic solvents compared to Ir(III) and Rh(III), and similar to uptake results, this trend was likely due to the lower -2 formal charge of $[\text{PtCl}_6]^{2-}$ and $[\text{IrCl}_6]^{2-}$. The uptake of 5 mM aqueous PGM salts with reduced ddFc (no oxidizer) was carried out, and despite no NOBF_4 oxidizer, 75 mg/g of Ir(IV) was reversibly extracted, while all other PGM salts showed negligible uptake. The reversible uptake of each PGM species with and without NOBF_4 oxidizer was shown in **Figure S33**. Iridium had a reversible redox couple $\text{IrCl}_6^{2-}/\text{IrCl}_6^{3-}$ with a formal potential of 0.65 V vs Ag/AgCl, which allowed Ir(IV) to spontaneously oxidize ddFc to ddFc^+ ($E^0 = 0.41$ V vs Ag/AgCl) and simultaneously bind the now reduced Ir(III) to oxidized ddFc^+ . Therefore, it was possible to selectively capture H_2IrCl_6 using ddFc e-LLE spontaneously – requiring no energy or material consumption.

Continuous redox-mediated ion-selective extraction. A 20 mL/min stream of 5 mM $\text{KAu}(\text{CN})_2$ was continuously extracted and purified without chemical consumption using our e-LLE system (**Figure S13, S14, and S15**). The system consisted of three closed liquid loops, three simple solvent extraction columns, and an electrochemical flow cell with two flow paths separated by a CEM. 20 mL of 2 mM ddFc in DBM organic solvent was continuously cycled in a closed loop at 10 mL/min through three solvent extraction columns: the oxidizing column, the leach column, and the reducing column (**Figure 4a**). In the oxidizing column, ddFc was oxidized to the active binding extractant species, ddFc^+ , by a closed aqueous oxidizing loop of 10 mM I_3^- flowing at 20 mL/min, where the reduced iodide was electrochemically regenerated. After the oxidation to ddFc^+ , the organic extractant phase entered the leach column, alongside

the 20 mL/min aqueous gold leach stream, initially containing 10 mM $\text{KAu}(\text{CN})_2$. The 20 mL gold leach stream was continuously recirculated, and 92% of aqueous gold was extracted (**Figure S34**) with an impressive gold uptake of 1402 mg/g_{ddFc} achieved over the span of 8 hours (**Figure 4b**).

Following the leach column, the gold-laden organic phase passed through the final reducing column, where a 10 mL closed aqueous loop of 10 mM sodium ferrocyanide (20 mL/min) simultaneously reduced ddFc⁺ and extracted the now unbound $[\text{Au}(\text{CN})_2]^-$ anion into the aqueous reduction loop. The organic ddFc was then cycled back to the oxidation column to repeat the e-LLE process, thereby forming a closed extractant loop that does not consume extractant or solvent. All extracted gold was ultimately sequestered to the closed aqueous reduction loop, where it was concentrated. 91% of the extracted gold was reversibly recovered (**Figure 4b**) and up-concentrated by a factor of 2, and 3.7 gold molecules were extracted per ddFc molecule – proving that ddFc extractant was indeed recycled and reused (**Figure S34**).

Lastly, the spent iodine oxidizing agent and ferrocyanide reducing agent were electrochemically regenerated in a CEM-separated flow cell with 4x4x0.3 cm carbon felt electrodes – a similar configuration to a redox flow battery⁵²⁻⁵⁴. The cell was operated with a constant current of 2 mA until a two-electrode potential of 0.23V ($E_{\text{ox}} - E_{\text{red}}$) was reached, and the potential was held constant thereafter (**Figure S35**). Due to the low operating potential <0.23 V and operating current <2 mA, coupled with the high molar utilization of ddFc (3.7 mol Au/ddFc), energy consumption per gold recovered was 0.143 kJ/g_{Au} (**Figure 4c**), which was

lower than our previous PVF-CNT work²⁰ by a factor of 75 (98.7% reduction in energy consumption). In terms of cost, our continuous e-LLE system had a total energy cost of \$2.89 per metric ton of gold recovered, with no materials consumed. For perspective, the solar cell from a pocket calculator (5 cm², 3 mW power) could recover 2.2 grams of pure gold per day with our unoptimized bench-scale e-LLE proof of concept system.

Evaluation of e-LLE for real metal leach streams. 310 grams of locally sourced electronic waste in the form of DDR3 computer RAM modules were added to 1 L of 10 mM KCN to leach the surface gold and other metals, following the optimized leaching procedure of our previous work²⁰. The leach process was optimized to minimize chemical consumption. After 24 hours of aerated leaching, the e-waste leach solution contained 2.11 g/L copper, 676.53 mg/L nickel, 309.89 mg/L gold, 1.94 mg/L iron, and 0.13 mg/L silver as the 5 major constituents (**Figure S36a**), and the leach solution had a pH of 10. Without any further processing of the leach solution, the gold was recovered with our e-LLE process with 2 mM ddFc electro-extractant with a gold uptake of 109 mg/g (**Figure S36b**), and when compared to the pure gold absorption isotherm in **Figure 3d**, gold uptake from e-waste leach was 30% lower, and this loss in uptake was likely due to the 29 – fold molar excess of competing copper and nickel ions in the leach solution. When the organic phase ddFc⁺ was reduced with 10 mM of aqueous ferrocyanide, 91.6% of extracted gold was released into the aqueous reducing phase, and the gold was successfully purified from 9.9% to a final gold purity of 59.6% in a single extraction pass (**Figure 5a**), with a gold selectivity factor of 13.3:1 relative to Cu, Ni, Fe, and Ag, proving that selective

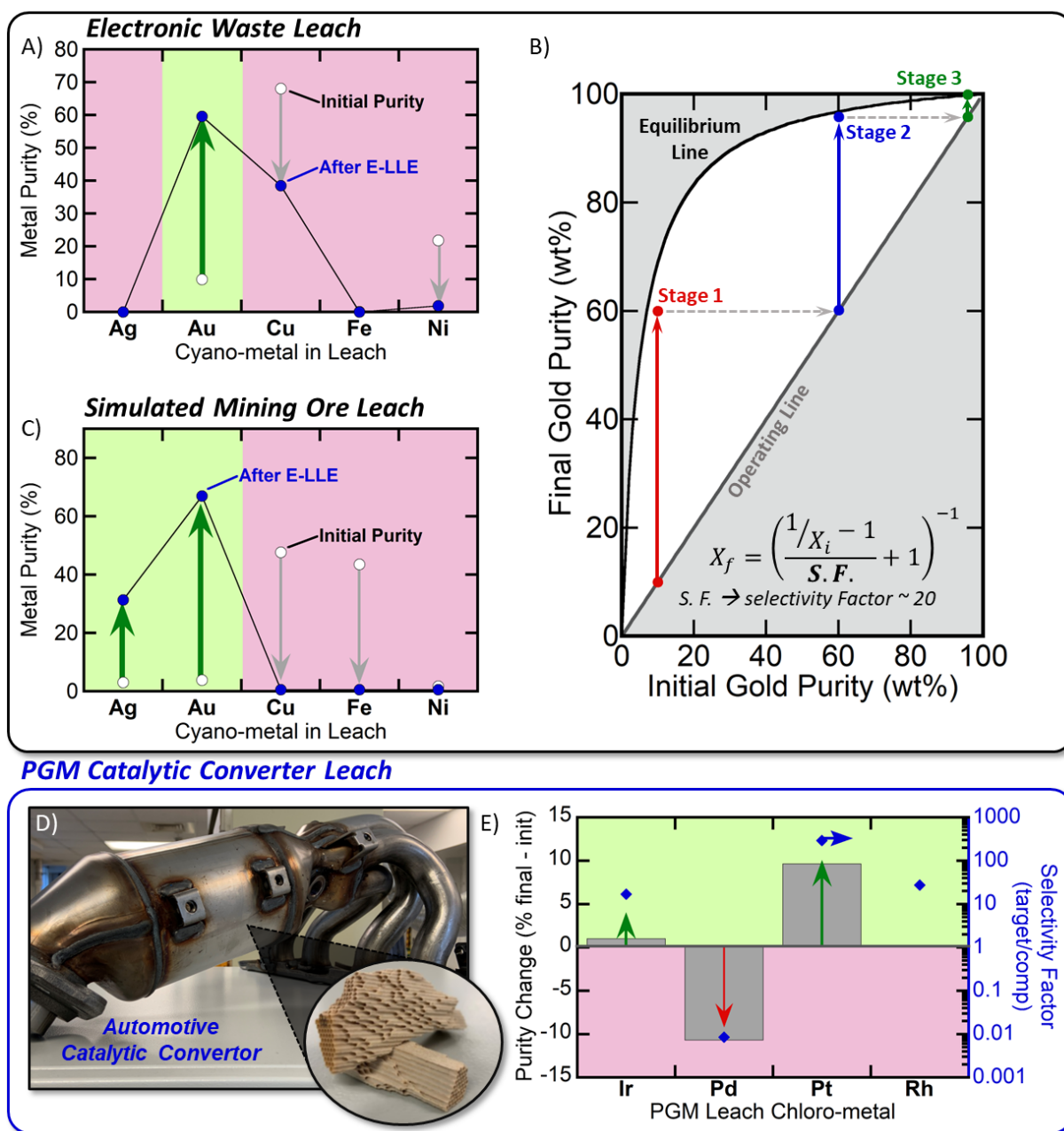


Figure 5. A) Comparison of the initial metal purity (white) of a gold leach solution from electronic waste and final purity (blue) obtained after e-LLE extraction. Only the purity of gold increased. B) A McCabe Thiele plot for E-LLE where the upper equilibrium line was constructed from the shown equation using the gold selectivity factor relative to silver, copper, nickel, and iron. The electronic waste leach solution containing 10% gold was purified with three consecutive E-LLE stages, where the purity was brought to 60% in the first stage (red), 91% in the second stage (blue), and finally 99.8% in the third stage (green). C) Comparison of the initial metal purity (white) of a gold leach solution from simulated mining ore and final purity (blue) obtained after e-LLE extraction. The purity of gold increased most. D) Image of the 2014 Scion Tc catalytic converter and the monolithic catalyst structure that PGMs were extracted from to produce a real-world PGM leach solution. E) The experimental results of E-LLE extraction of PGMs from the catalyst converter leach solution. The grey bars represent the change in metal purity following E-LLE, and the blue diamonds represent the selectivity factor of ddFc.

recovery and purification of gold was possible with real-world e-waste leach solutions with

the ddFc electro-extractant e-LLE system.

Gold in the e-waste leach solution was further purified by consecutive extractions using the E-LLE approach, where the first extraction stage brought gold purity from 10% to 60.1%, a second extraction increased purity to 91.4%, and a third extraction brought the final gold purity to 99.8% (**Figure 5b**). A McCabe Thiele plot was constructed from the multi-stage E-LLE experimental results, and the e-LLE equilibrium line was constructed from the system mass balance and the average gold selectivity factor of 20 (relative to Ag, Cu, Fe, and Ni competing species), and the resulting **Figure 5b**, showed that experimental multi-stage performance was captured within 5% error using the McCabe Thiele graphical approximation method for the theoretical number of separation stages. Therefore, **Figure 5b** may be used as a process design roadmap to predict the number of consecutive E-LLE stages required to achieve a particular gold purity, and using this method, bullion grade gold (99.99% pure) could be achieved from 10% gold e-waste leach in a total of 4 E-LLE stages.

A simulated gold ore leach solution was synthesized following previous methods in literature²⁰, resulting in a solution containing 21.17 mg/L Cu, 19.31 mg/L Fe, 1.73 mg/L Au, 1.37 mg/L Ag, and 0.78 mg/L Ni. After e-LLE extraction with 2 mM ddFc, 98.3% of the gold contained in the leach solution was extracted (**Figure S36b**) with a relative selectivity factor of 50.1, and the purity of gold increased from 3.9% in the leach to a final gold purity of 67.0% (**Figure 5c**), demonstrating the applicability of our e-LLE approach for gold ore refinement.

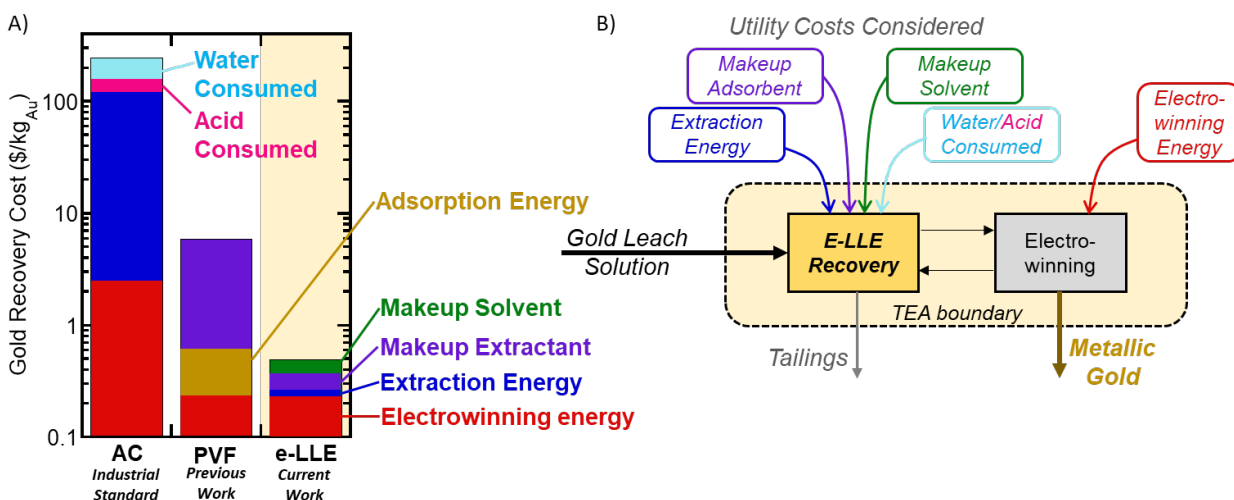


Figure 6. A) A gold refinement cost comparison and breakdown between three methods of gold recovery: AC - the industrial standard used in the CIP process, PVF-CNT electrosorption – our previous work, and ddFc e-LLE extraction. Note the y-axis is logarithmic. B) Schematic of all inputs and outputs within the boundary of this technoeconomic analysis.

Lastly, a real PGM leach solution was generated from the digestion of an automotive catalytic converter (2014 Scion Tc), and PGM purification was carried out with e-LLE. The new 2014 Scion Tc catalyst material was ground and leached with chlorine gas as the oxidizer and Cl⁻ as the stabilizing ligand resulting in an acidic aqueous solution containing trace anionic chloro-PGM complexes (0.92 mg/L Ir, 0.46 mg/L Pt, and 0.03 mg/L Rh), with the major species being palladium at 1471.6 mg/L. Despite high initial palladium concentration, iridium and platinum were the only two PGM species to increase in purity after e-LLE (**Figure 5e**), where platinum increased from 0.1% to 9.7% pure in a single extraction stage, and a platinum selectivity factor of 294 relative to Pd + Ir + Rh was achieved. Therefore, the e-LLE system demonstrated selective purification of platinum from a real-world PGM leach stream.

Technoeconomic Analysis. The technoeconomics of our e-LLE system were evaluated and compared to the industrial standard technology, activated carbon-based CIP³³, and compared

to our previous work utilizing PVF-CNT electrode adsorbent. The scope of this techno-economic analysis covered all processing of the gold stream following the cyanide leaching stage, including the recovery and concentration of gold in solution and gold electrodeposition (or electrowinning) (**Figure 6b**). From a basis of 4000 L/min leach solution flow containing 50% gold and silver at a concentration ranging from 0.006 to 1000 mg/L gold, the energy and materials costs were estimated for each recovery method, CIP, PVF electrosorption, and e-LLE, utilizing a 6 capture unit cascade model that recovered 99.6% of gold from the leach solution²⁰. For the e-LLE system, the cost to make up the 0.1% of solvent, and 0.5% of ddFc lost to the aqueous tailings stream was dominant cost factor at an initial gold leach concentration below 10 mg/L (low grade ore mining conditions), justifying the selection of solvent and extractant with high immiscibility in water (**Figure 6x**). At gold feed concentration above 10 mg/L, the energy cost of gold electrodeposition was dominant, and the energy cost of continuously extracting gold with ddFc was lowest, making up 10% of the total operational cost of ddFc due to the low 0.86 kJ/g_{Au} energy consumption of the e-LLE process (**Figure 6a**). At a gold feed concentration of 100 mg/L, our ddFc system cost \$0.49 USD per kg of gold recovered, compared to \$5.90 per kg for PVF electrosorption, and \$245 per kg for conventional activated carbon (**Figure 6a**). Therefore, the e-LLE system can be >500 times lower cost than the current industrial process, CIP, by consuming over 99.9% less energy, and 99.4% less chemical materials. Conventional AC was estimated to consume 14,000 Liters of fresh water per kg of gold recovered, accounting for 35% of the total utility cost (\$87/kg_{Au}). In addition, the high selectivity of the e-LLE process resulted in 99.2% pure gold, where CIP

resulted in 50% gold requiring further costly processing not covered in this analysis. Lastly, the e-LLE process is a true, fully continuous process unlike CIP, simplifying the overall process design, reducing process size, technician count, and system downtime²⁸. Therefore, the continuous e-LLE process with ddFc extractant was predicted to be a highly economical method for sustainable gold recovery.

Conclusion. For the first time, we demonstrate a fully continuous approach to selective electrochemical separation utilizing ddFc electro-extractant, for eLLE and redox flow battery architecture for continuous electrochemical regeneration of redox mediating species iodine and ferrocyanide. A redox-mediated ddFc extractant was found to selectively extract gold, platinum, and iridium with highly enhanced molar utilization of the ferrocenium (> 89%), while retaining > 99 gold recovery efficiency owing to the continuous nature of the e-LLE system design. Coupled with reducing and oxidizing redox mediators with a low 0.23V overall working potential, the energy consumption of ddFc e-LLE was over 3 orders of magnitude lower than conventional CIP ($E_{\text{ddFc}} = 0.86 \text{ kJ/g}_{\text{Au}}$, $E_{\text{CIP}} = 2046 \text{ kJ/g}_{\text{Au}}$), and ddFc was observed to be highly selective to gold (> 20:1) and capable of simultaneous gold purification to over 99% and up-concentration by a factor of 16. ddFc was observed to preferentially bind to metal anions of increasing atomic mass, i.e., $\text{Au} > \text{Pt} \sim \text{Ir} > \text{Ag} > \text{Ru} > \text{Cu}$, and uptake decreased as the formal charge of the target anion becomes more negative, i.e., $[\text{Au}(\text{CN})_2]^- > [\text{PtCl}_6]^{2-} > [\text{IrCl}_6]^{3-}$. The e-LLE system was successful at purifying gold from real electronic waste and mining leach solution containing over 39 – fold excess metals.

The selectivity of ddFc to precious metals platinum, iridium, and rhodium were also investigated, and we concluded that ddFc preserves the exceptional binding selectivity of the single site redox-centers^{16, 19}. Real world precious metal leach streams were produced from electronic waste, simulated gold mining ore, and automotive catalytic converter material, and the e-LLE process was capable of purifying gold, platinum, and iridium directly, demonstrating real applicability for this technology. Lastly, the e-LLE system was operated fully continuously, simultaneously extracting and releasing gold autonomously, to achieve over 1500 mg/g uptake, over 90% gold removal, and 91% gold recovery efficiency, demonstrating a clear step forward in simplicity and performance of gold recovery over other methods. A technoeconomic analysis further indicated that the economics of ddFc e-LLE were very favorable (\$0.49 USD/kg_{Au}). From our work we believe that electrified liquid-liquid extraction with electrochemically switchable extractant, ddFc, presents a step-change in the design and advances of electrochemical separations as a sustainable, continuous, and economical means for the recovery and recycle of precious metals and will be the subject of future research for years to come.

ASSOCIATED CONTENT

The supporting information contains additional details on materials characterization, supplementary data, and experimental protocols.

AUTHOR INFORMATION

Corresponding author: x2su@illinois.edu

Notes

The authors declare no competing financial interest.

ACKNOWLEDGMENT

This material is based upon work supported by the U.S. Department of Energy, Office of Basic Energy Sciences under Award Number DOE DE-SC0021409.

REFERENCES

1. Srimuk, P.; Su, X.; Yoon, J.; Aurbach, D.; Presser, V., Charge-transfer materials for electrochemical water desalination, ion separation and the recovery of elements. *Nature Reviews Materials* **2020**, *5* (7), 517-538.
2. Alkhadra, M. A.; Su, X.; Suss, M. E.; Tian, H.; Guyes, E. N.; Shocron, A. N.; Conforti, K. M.; de Souza, J. P.; Kim, N.; Tedesco, M.; Khoiruddin, K.; Wenten, I. G.; Santiago, J. G.; Hatton, T. A.; Bazant, M. Z., Electrochemical Methods for Water Purification, Ion Separations, and Energy Conversion. *Chemical Reviews* **2022**, *122* (16), 13547-13635.
3. Su, X.; Tan, K.-J.; Elbert, J.; Rüttiger, C.; Gallei, M.; Jamison, T. F.; Hatton, T. A., Asymmetric Faradaic systems for selective electrochemical separations. *Energy & Environmental Science* **2017**, *10* (5), 1272-1283.
4. Harper, G.; Sommerville, R.; Kendrick, E.; Driscoll, L.; Slater, P.; Stolkin, R.; Walton, A.; Christensen, P.; Heidrich, O.; Lambert, S.; Abbott, A.; Ryder, K.; Gaines, L.; Anderson, P., Recycling lithium-ion batteries from electric vehicles. *Nature* **2019**, *575* (7781), 75-86.
5. Kim, K.; Raymond, D.; Candeago, R.; Su, X., Selective cobalt and nickel electrodeposition for lithium-ion battery recycling through integrated electrolyte and interface control. *Nat Commun* **2021**, *12* (1), 6554.
6. High, M.; Patzschke, C. F.; Zheng, L. Y.; Zeng, D. W.; Gavalda-Diaz, O.; Ding, N.; Chien, K. H. H.; Zhang, Z. L.; Wilson, G. E.; Berenov, A. V.; Skinner, S. J.; Campbell, K. L. S.; Xiao, R.; Fennell, P. S.; Song, Q. L., Precursor engineering of hydrotalcite-derived redox sorbents for reversible and stable thermochemical oxygen storage. *Nature Communications* **2022**, *13* (1).
7. Li, X.; Zhao, X. H.; Liu, Y. Y.; Hatton, T. A.; Liu, Y. Y., Redox-tunable Lewis bases for electrochemical carbon dioxide capture. *Nature Energy* **2022**, *7* (11), 1065-1075.

8. Liu, Y. Y.; Ye, H. Z.; Diederichsen, K. M.; Van Voorhis, T.; Hatton, T. A., Electrochemically mediated carbon dioxide separation with quinone chemistry in salt-concentrated aqueous media. *Nature Communications* **2020**, *11* (1).
9. Cotty, S.; Jeon, J.; Elbert, J.; Jeyaraj, V. S.; Mironenko, A. V.; Su, X., Electrochemical recycling of homogeneous catalysts. *Sci. Adv.* **2022**, *8* (42).
10. Wilcox, J., An electro-swing approach. *Nature Energy* **2020**, *5* (2), 121-122.
11. Kim, N.; Elbert, J.; Kim, C.; Su, X., Redox-Copolymers for Nanofiltration-Enabled Electrodialysis. *ACS Energy Letters* **2023**, *8* (5), 2097-2105.
12. Kim, N.; Lee, J.; Su, X., Precision Tuning of Highly Selective Polyelectrolyte Membranes for Redox-Mediated Electrochemical Separation of Organic Acids. *Adv Funct Mater* **2023**, *33* (12), 2211645.
13. Su, X.; Chen, Z.; St-Pierre, J.; Vasiljevic, N., Electrochemistry for Recycling. *The Electrochemical Society Interface* **2021**, *30* (3), 41-43.
14. Chen, R.; Sheehan, T.; Ng, J. L.; Brucks, M.; Su, X., Capacitive deionization and electrosorption for heavy metal removal. *Environmental Science: Water Research & Technology* **2020**, *6* (2), 258-282.
15. Su, X.; Hatton, T. A., Redox-electrodes for selective electrochemical separations. *Advances in Colloid and Interface Science* **2017**, *244*, 6-20.
16. Chen, R. L.; Feng, J. Y.; Jeon, J.; Sheehan, T.; Ruttiger, C.; Gallei, M.; Shukla, D.; Su, X., Structure and Potential-Dependent Selectivity in Redox-Metallopolymers: Electrochemically Mediated Multicomponent Metal Separations. *Adv Funct Mater* **2021**, *31* (15).
17. Kim, K.; Candeago, R.; Rim, G.; Raymond, D.; Park, A.-H. A.; Su, X., Electrochemical approaches for selective recovery of critical elements in hydrometallurgical processes of complex feedstocks. *iScience* **2021**, *24* (5), 102374.
18. Candeago, R.; Kim, K.; Vapnik, H.; Cotty, S.; Aubin, M.; Berensmeier, S.; Kushima, A.; Su, X., Semiconducting Polymer Interfaces for Electrochemically Assisted Mercury Remediation. *Acs Appl Mater Inter* **2020**, *12* (44), 49713-49722.
19. Cotty, S.; Jeon, J.; Elbert, J.; Jeyaraj, V. S.; Mironenko, A. V.; Su, X., Electrochemical recycling of homogeneous catalysts. *Sci. Adv.* **2022**, *8* (42), 12.
20. Cotty, S. R.; Kim, N.; Su, X., Electrochemically Mediated Recovery and Purification of Gold for Sustainable Mining and Electronic Waste Recycling. *ACS Sustainable Chemistry & Engineering* **2023**, *11* (9), 3975-3986.
21. Guo, Z.-Y.; Ji, Z.-Y.; Wang, J.; Chen, H.-Y.; Liu, J.; Zhao, Y.-Y.; Li, F.; Yuan, J.-S., Development of electrochemical lithium extraction based on a rocking chair system of LiMn₂O₄/Li_{1-x}Mn₂O₄: Self-driven plus external voltage driven. *Separation and Purification Technology* **2021**, *259*, 118154.
22. Xu, T.; Huang, C., Electrodialysis-based separation technologies: A critical review. *AIChE Journal* **2008**, *54* (12), 3147-3159.
23. Brown, C. G.; Sherrington, L. G., Solvent extraction used in industrial separation of rare earths. *Journal of Chemical Technology and Biotechnology* **1979**, *29* (4), 193-209.

24. El-Nadi, Y. A., Solvent Extraction and Its Applications on Ore Processing and Recovery of Metals: Classical Approach. *Separation & Purification Reviews* **2017**, *46* (3), 195-215.
25. Mooiman, M. B. In *THE SOLVENT-EXTRACTION OF PRECIOUS METALS - A REVIEW*, 17th International Precious Metals Conference, Newport, Ri, Jun; Newport, Ri, 1993; pp 411-434.
26. Yordanov, A. T.; Roundhill, D. M., Solution extraction of transition and post-transition heavy and precious metals by chelate and macrocyclic ligands. *Coordination Chemistry Reviews* **1998**, *170*, 93-124.
27. Mahandra, H.; Faraji, F.; Ghahreman, A., Novel Extraction Process for Gold Recovery from Thiosulfate Solution Using Phosphonium Ionic Liquids. *ACS Sustainable Chemistry & Engineering* **2021**, *9*(24), 8179-8185.
28. Towler, G.; Sinnott, R., Chapter 17 - Separation columns (distillation, absorption, and extraction). In *Chemical Engineering Design (Third Edition)*, Towler, G.; Sinnott, R., Eds. Butterworth-Heinemann: 2022; pp 631-733.
29. Kislik, V. S., Chapter 3 - Chemistry of Metal Solvent Extraction. In *Solvent Extraction*, Kislik, V. S., Ed. Elsevier: Amsterdam, 2012; pp 113-156.
30. Long, J.; Rice, J. L., Climate urbanism: crisis, capitalism, and intervention. *Urban Geography* **2021**, *42* (6), 721-727.
31. Gjorgievski, V. Z.; Mihajloska, E.; Abazi, A.; Markovska, N., Sustainable Development Goals-Climate Action Nexus:Quantification of Synergies and Trade-offs. *Clean Technol. Environ. Policy* **2022**, *24* (1), 303-313.
32. Moreau, V.; Dos Reis, P. C.; Vuille, F., Enough Metals? Resource Constraints to Supply a Fully Renewable Energy System. *Resources-Basel* **2019**, *8* (1), 18.
33. Calvo, G.; Mudd, G.; Valero, A.; Valero, A., Decreasing Ore Grades in Global Metallic Mining: A Theoretical Issue or a Global Reality? *Resources* **2016**, *5* (4), 36.
34. Craig, J. R.; Rimstidt, J. D., Gold production history of the United States. *Ore Geol. Rev.* **1998**, *13* (6), 407-464.
35. Fischer-Kowalski, M.; Swilling, M., *Decoupling Natural Resource Use and Environmental Impacts from Economic Growth*. 2011.
36. Vidal, O., 3 - Energy Requirements of the Mining and Metallurgical Industries. In *Mineral Resources and Energy*, Vidal, O., Ed. Elsevier: 2018; pp 27-52.
37. Sovacool, B. K.; Ali, S. H.; Bazilian, M.; Radley, B.; Nemery, B.; Okatz, J.; Mulvaney, D., Sustainable minerals and metals for a low-carbon future. *Science* **2020**, *367*(6473), 30-33.
38. Butt, C. R. M.; Hough, R. M., Why Gold is Valuable. *Elements* **2009**, *5* (5), 277-280.
39. Murphy, K., Gold RRS 2022 — Surge in recent discoveries. 3 MAr, 2022 ed.; S&P Global Market Intelligence: 2022.
40. Cui, J. R.; Zhang, L. F., Metallurgical recovery of metals from electronic waste: A review. *Journal of Hazardous Materials* **2008**, *158* (2-3), 228-256.

41. Zadra, J. B.; Engel, A. L.; Heinen, H. J., *Process for Recovering Gold and Silver from Activated Carbon by Leaching and Electrolysis*. U.S. Department of the Interior, Bureau of Mines: 1952.
42. Ford, P.; Santos, E.; Ferrao, P.; Margarido, F.; Van Vliet, K. J.; Olivetti, E., Economics of End-of-Life Materials Recovery: A Study of Small Appliances and Computer Devices in Portugal. *Environ Sci Technol* **2016**, *50* (9), 4854-4862.
43. Beyuo, M.; Abaka-Wood, G. In *ZADRA Elution Circuit Optimisation and Operational Experience at the CIL Plant of Gold Fields Ghana Limited*, 4th UMaT Bienn. Int. Min. Miner. Conf., 2016; pp 161-167.
44. Cutting cobalt. *Nature Energy* **2020**, *5* (11), 825-825.
45. Babu, B. R.; Parande, A. K.; Basha, C. A., Electrical and electronic waste: a global environmental problem. *Waste Manage. Res.* **2007**, *25* (4), 307-318.
46. Ding, Y. J.; Zhang, S. E.; Liu, B.; Zheng, H. D.; Chang, C. C.; Ekberg, C., Recovery of precious metals from electronic waste and spent catalysts: A review. *Resources Conservation and Recycling* **2019**, *141*, 284-298.
47. Yu, M. L.; Wang, K.; Vredenburg, H., Insights into low-carbon hydrogen production methods: Green, blue and aqua hydrogen. *International Journal of Hydrogen Energy* **2021**, *46* (41), 21261-21273.
48. Papageorgiou, N.; Maier, W. F.; Grätzel, M., An Iodine/Triiodide Reduction Electrocatalyst for Aqueous and Organic Media. *Journal of The Electrochemical Society* **1997**, *144* (3), 876.
49. Masahiro, T.; Akitsugu, O.; Taijiro, O., The Chemical Behavior of Low Valence Sulfur Compounds. VIII. The Oxidation of Sodium Thiosulfate with Ozone. *Bulletin of the Chemical Society of Japan* **1973**, *46* (12), 3785-3789.
50. Rumble, J. R., *CRC handbook of chemistry and physics*. 98th ed.; CRC Press: Boca Raton, FL, 2017.
51. Sarla, M.; Pandit, M.; Tyagi, D. K.; Kapoor, J. C., Oxidation of cyanide in aqueous solution by chemical and photochemical process. *Journal of Hazardous Materials* **2004**, *116* (1), 49-56.
52. Pei, Z. B.; Zhu, Z. X.; Sun, D.; Cai, J. Y.; Mosallanezhad, A.; Chen, M. H.; Wang, G. M., Review of the I³/I² redox chemistry in Zn-iodine redox flow batteries. *Materials Research Bulletin* **2021**, *141*.
53. Li, X.; Gao, P. Y.; Lai, Y. Y.; Bazak, J. D.; Hollas, A.; Lin, H. Y.; Murugesan, V.; Zhang, S. Y.; Cheng, C. F.; Tung, W. Y.; Lai, Y. T.; Feng, R. Z.; Wang, J.; Wang, C. L.; Wang, W.; Zhu, Y., Symmetry-breaking design of an organic iron complex catholyte for a long cyclability aqueous organic redox flow battery. *Nature Energy* **2021**, *6* (9), 873-881.
54. Orita, A.; Verde, M. G.; Sakai, M.; Meng, Y. S., A biomimetic redox flow battery based on flavin mononucleotide. *Nat Commun* **2016**, *7* (1), 13230.